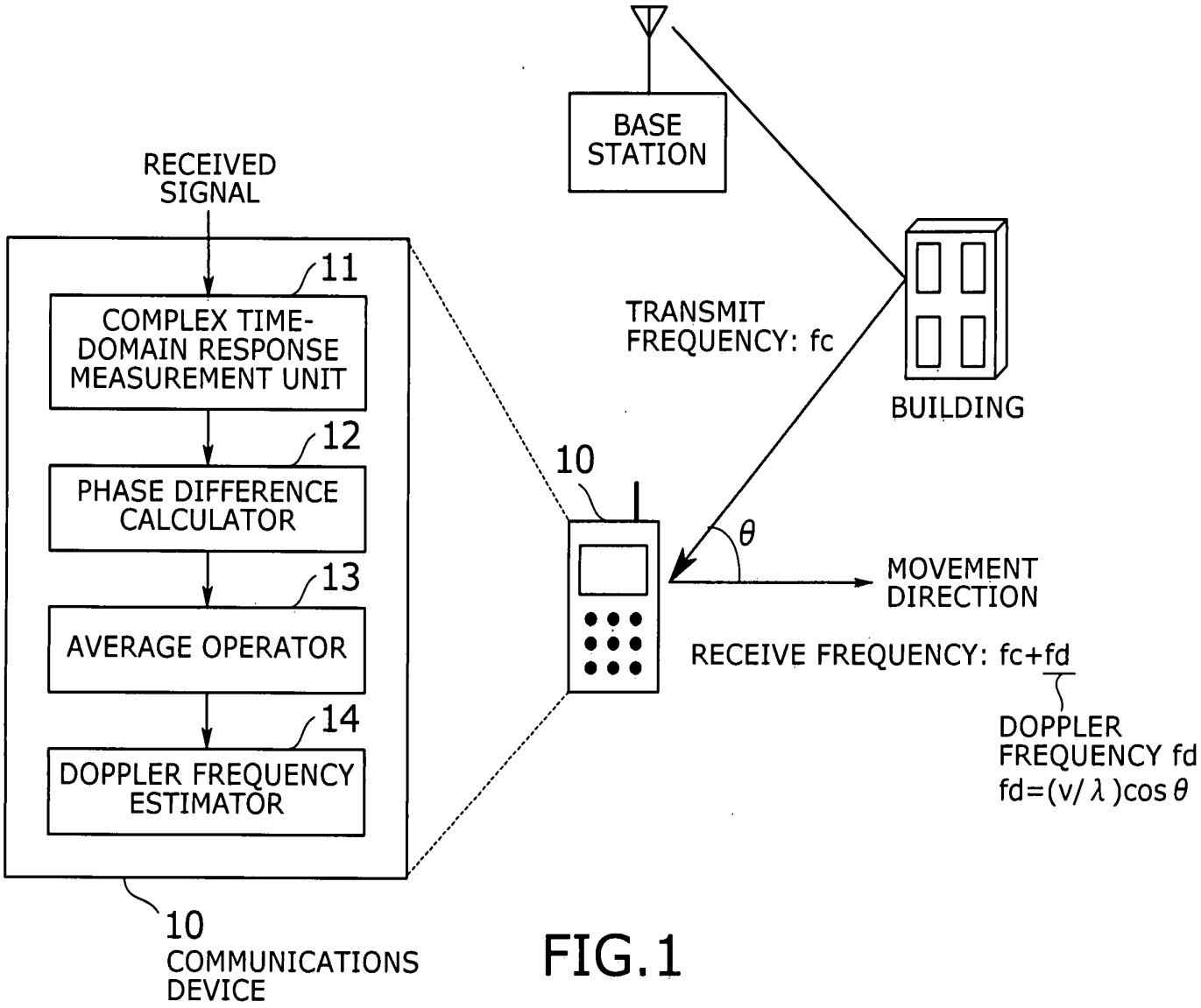
BASE STATION
RECEIVED SIGNAL
11
COMPLEX TIME-DOMAIN RESPONSE MEASUREMENT UNIT
12
PHASE DIFFERENCE CALCULATOR
13
AVERAGE OPERATOR
14
DOPPLER FREQUENCY ESTIMATOR
TRANSMIT FREQUENCY: fc
BUILDING
10
θ
MOVEMENT DIRECTION
RECEIVE FREQUENCY: fc+fd
DOPPLER FREQUENCY fd
fd=(v/λ)cosθ
10
COMMUNICATIONS DEVICE

FIG.1

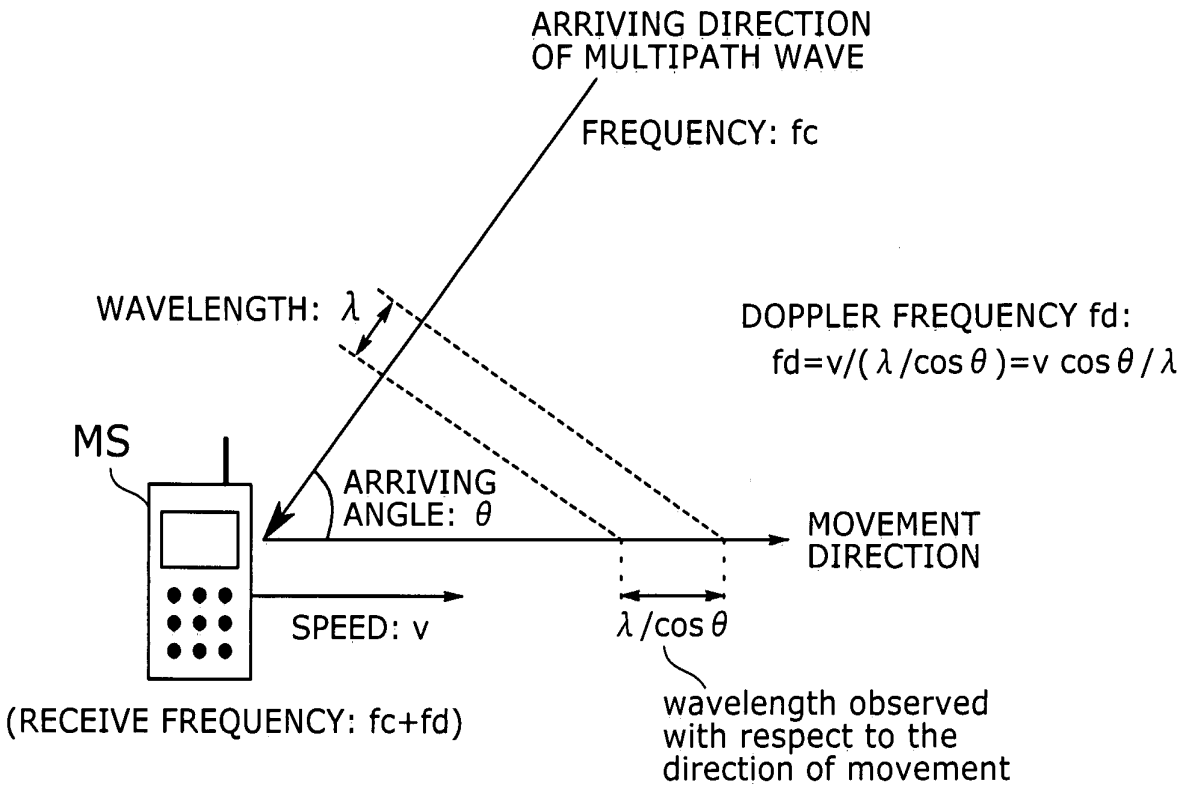
ARRIVING DIRECTION
OF MULTIPATH WAVE
FREQUENCY: fc
WAVELENGTH: λ
DOPPLER FREQUENCY fd:
fd=v/(λ/cosθ)=v cosθ/λ
MS
ARRIVING
ANGLE: θ
MOVEMENT
DIRECTION
SPEED: v
λ/cosθ
(RECEIVE FREQUENCY: fc+fd)
wavelength observed
with respect to the
direction of movement

FIG.2

FIG. 3A

Radio waves come from the same direction as or opposite direction to the mobile station's movement. This situation maximizes Doppler frequency shift.

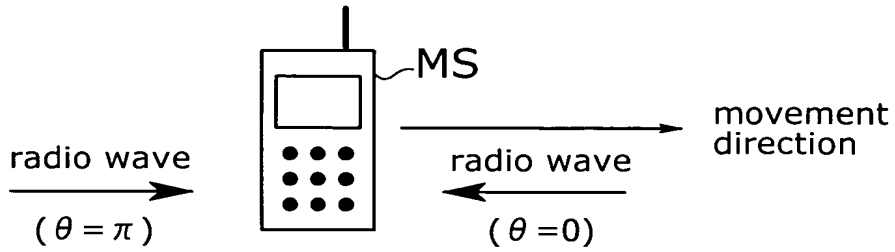

FIG. 3B

Radio waves come from the direction perpendicular to the mobile station's movement. No Doppler frequency shift occurs in this condition.

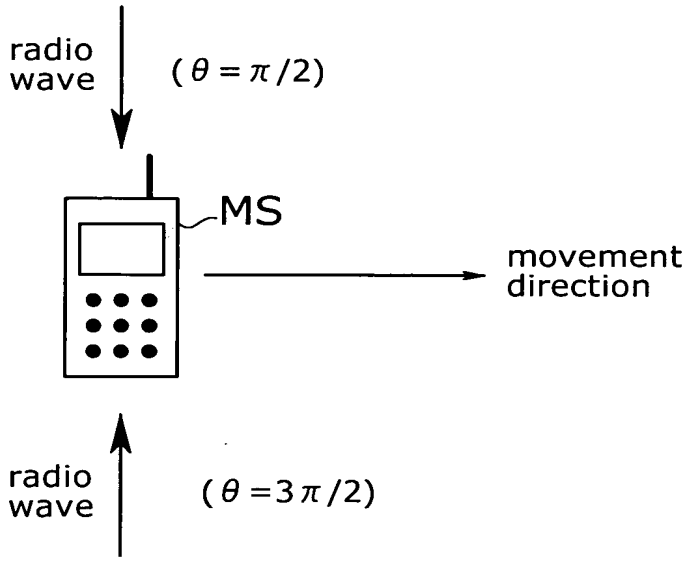

FIG. 4A

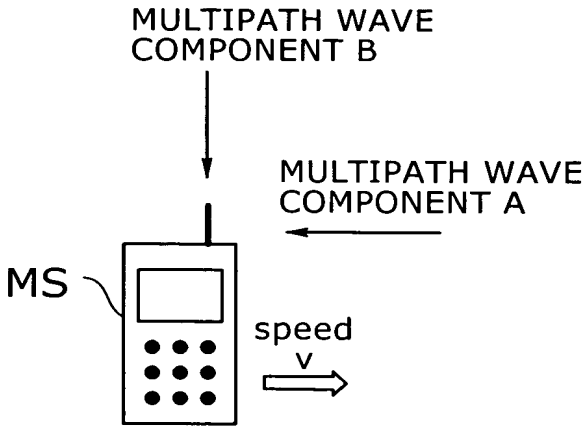
MULTIPATH WAVE
COMPONENT B
MULTIPATH WAVE
COMPONENT A
MS
speed
v

FIG. 4B

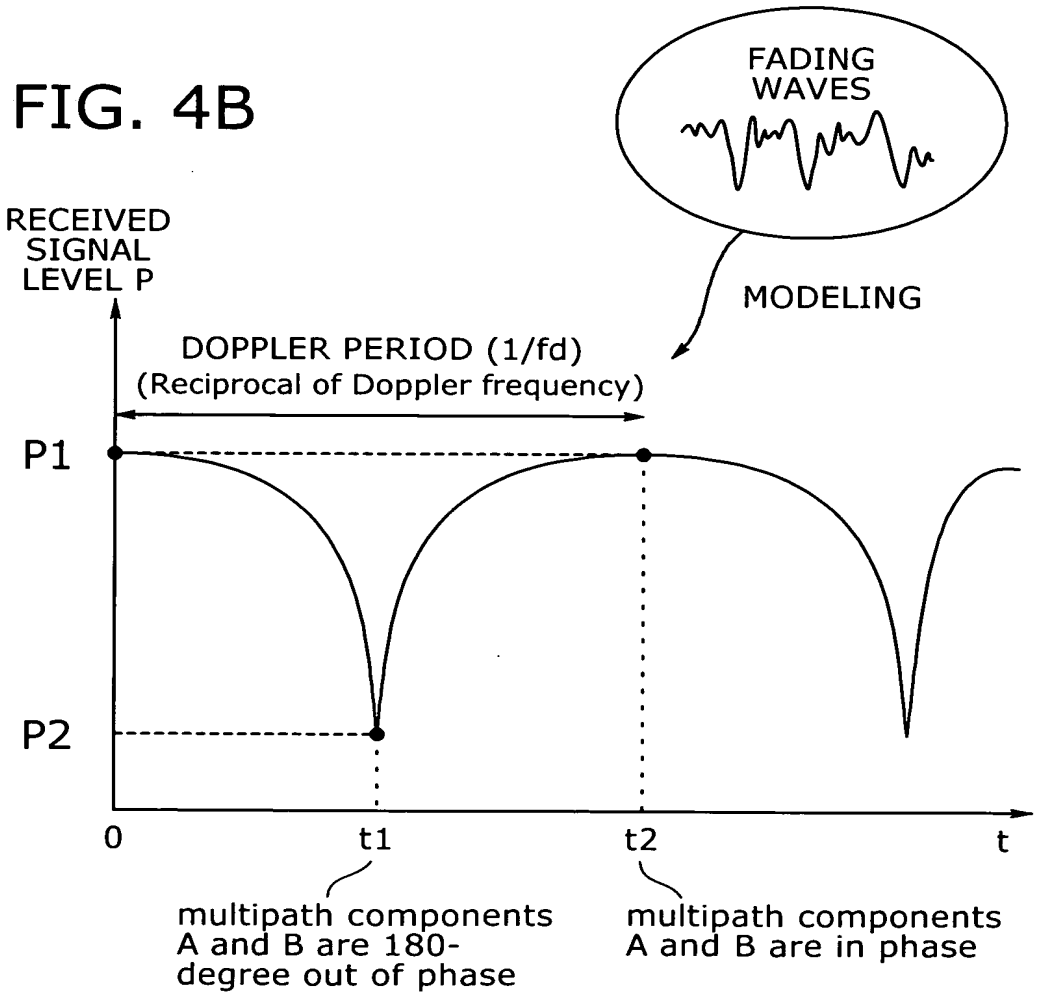
FADING
WAVES
MODELING
RECEIVED
SIGNAL
LEVEL P
DOPPLER PERIOD (1/fd)
(Reciprocal of Doppler frequency)
P1
P2
0
t1
t2
t
multipath components
A and B are 180-
degree out of phase
multipath components
A and B are in phase

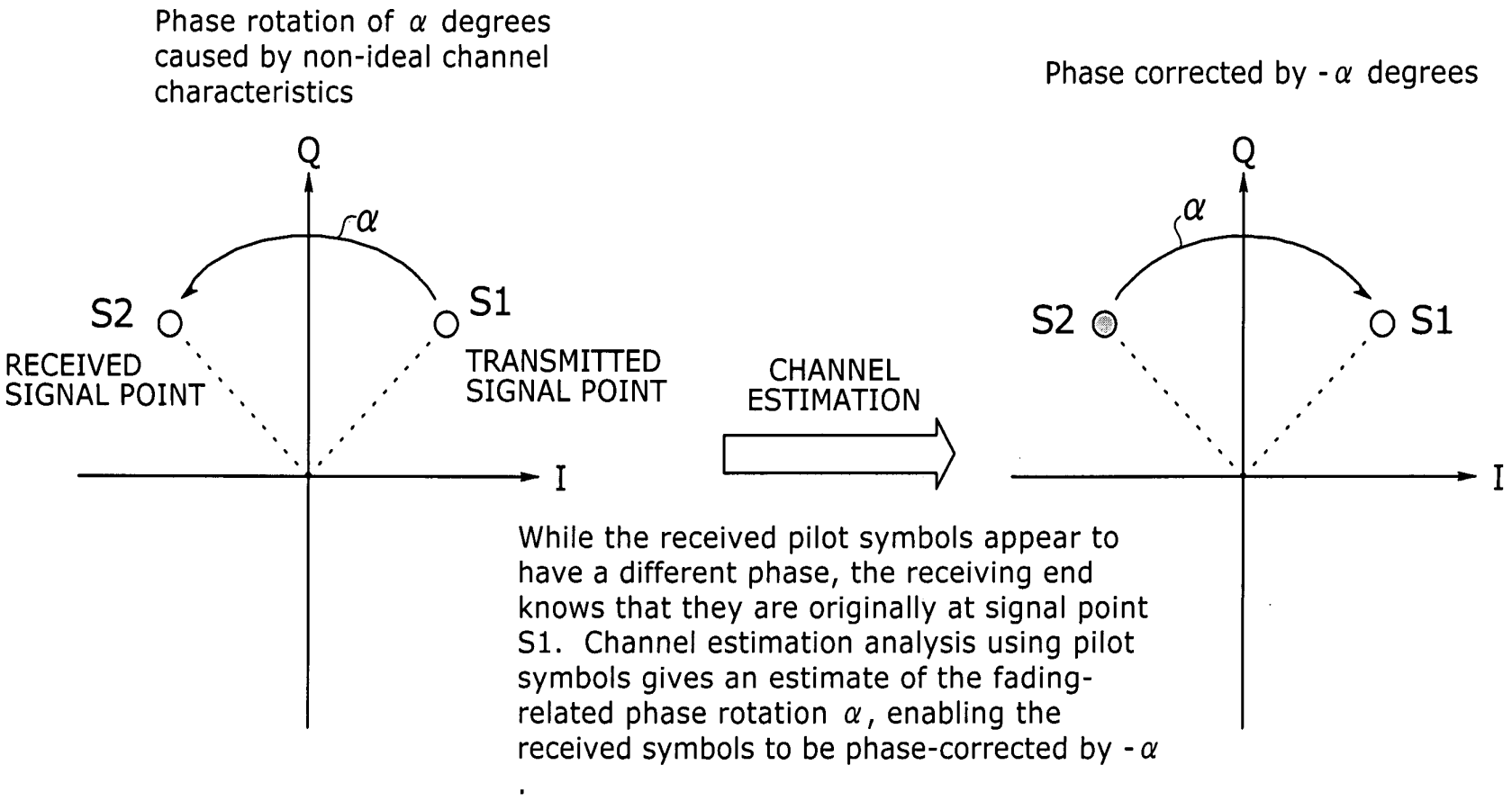
Phase rotation of α degrees caused by non-ideal channel characteristics
Q
α
S2
S1
RECEIVED SIGNAL POINT
TRANSMITTED SIGNAL POINT
I
CHANNEL ESTIMATION
Phase corrected by - α degrees
Q
α
S2
S1
I
While the received pilot symbols appear to have a different phase, the receiving end knows that they are originally at signal point S1. Channel estimation analysis using pilot symbols gives an estimate of the fading-related phase rotation α, enabling the received symbols to be phase-corrected by - α

FIG. 5

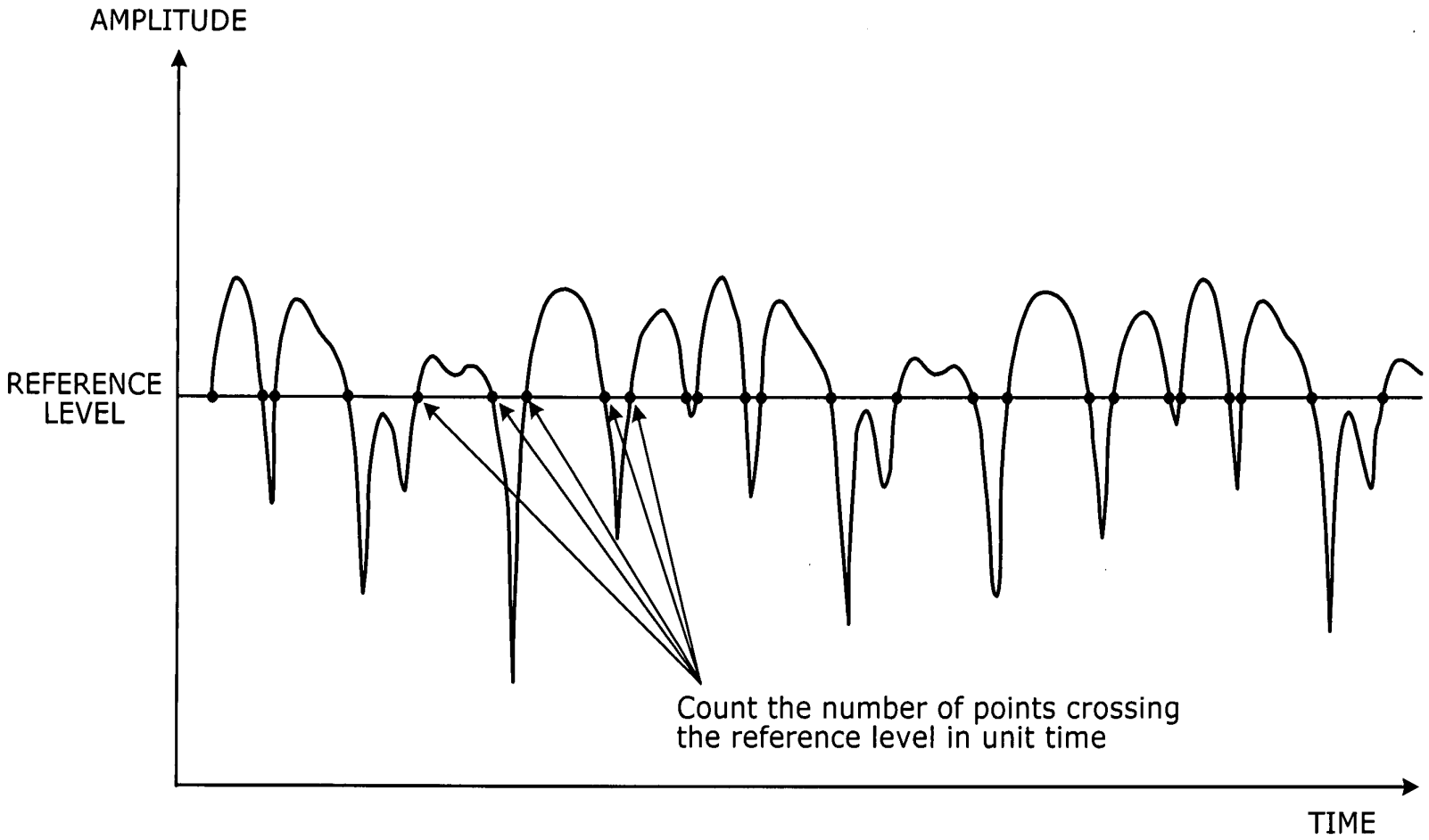

PRIOR ART

FIG.6

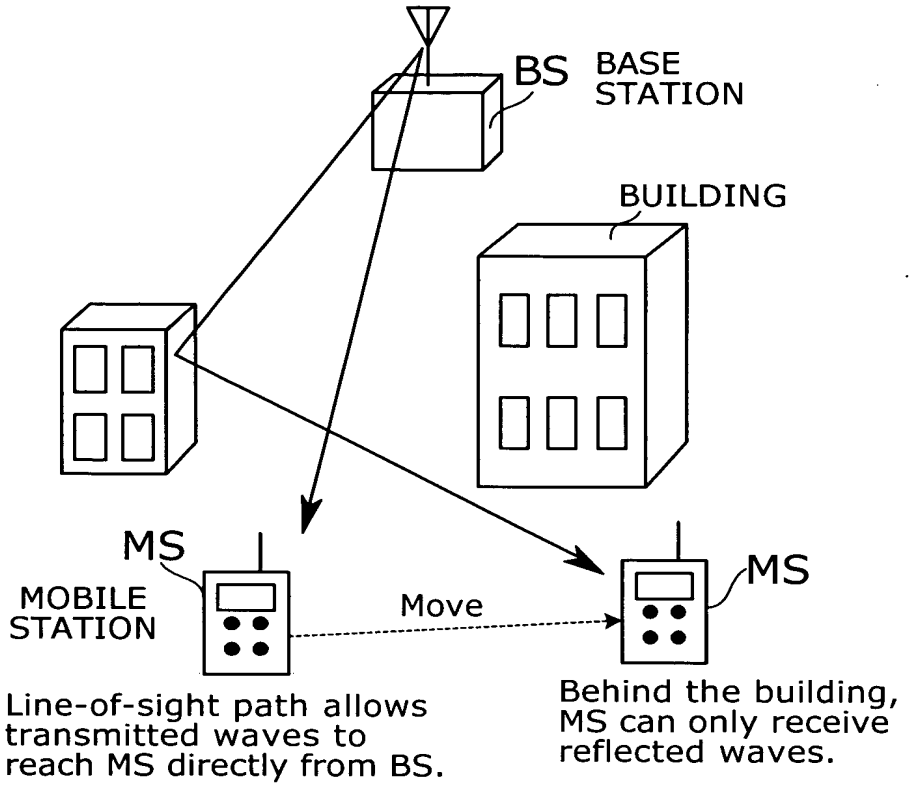
BS
BASE STATION
BUILDING
MS
MOBILE STATION
Move
MS
Line-of-sight path allows transmitted waves to reach MS directly from BS.
Behind the building, MS can only receive reflected waves.

FIG.7A

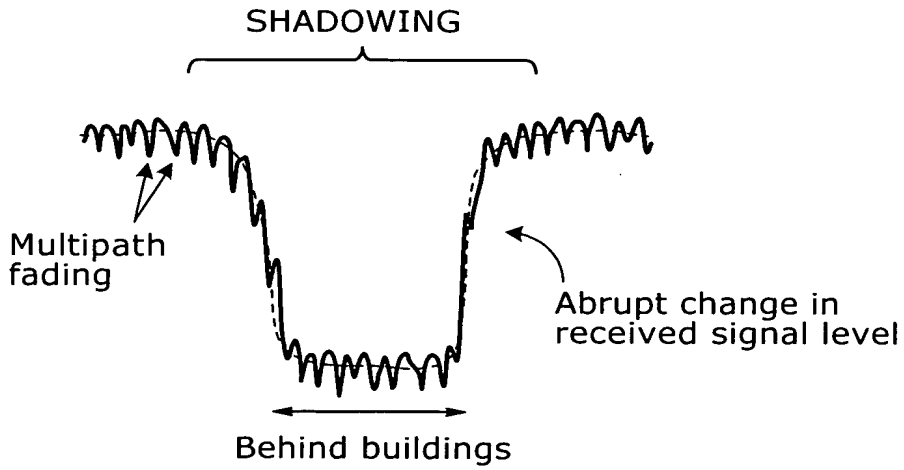
SHADOWING
Multipath fading
Abrupt change in received signal level
Behind buildings

FIG.7B

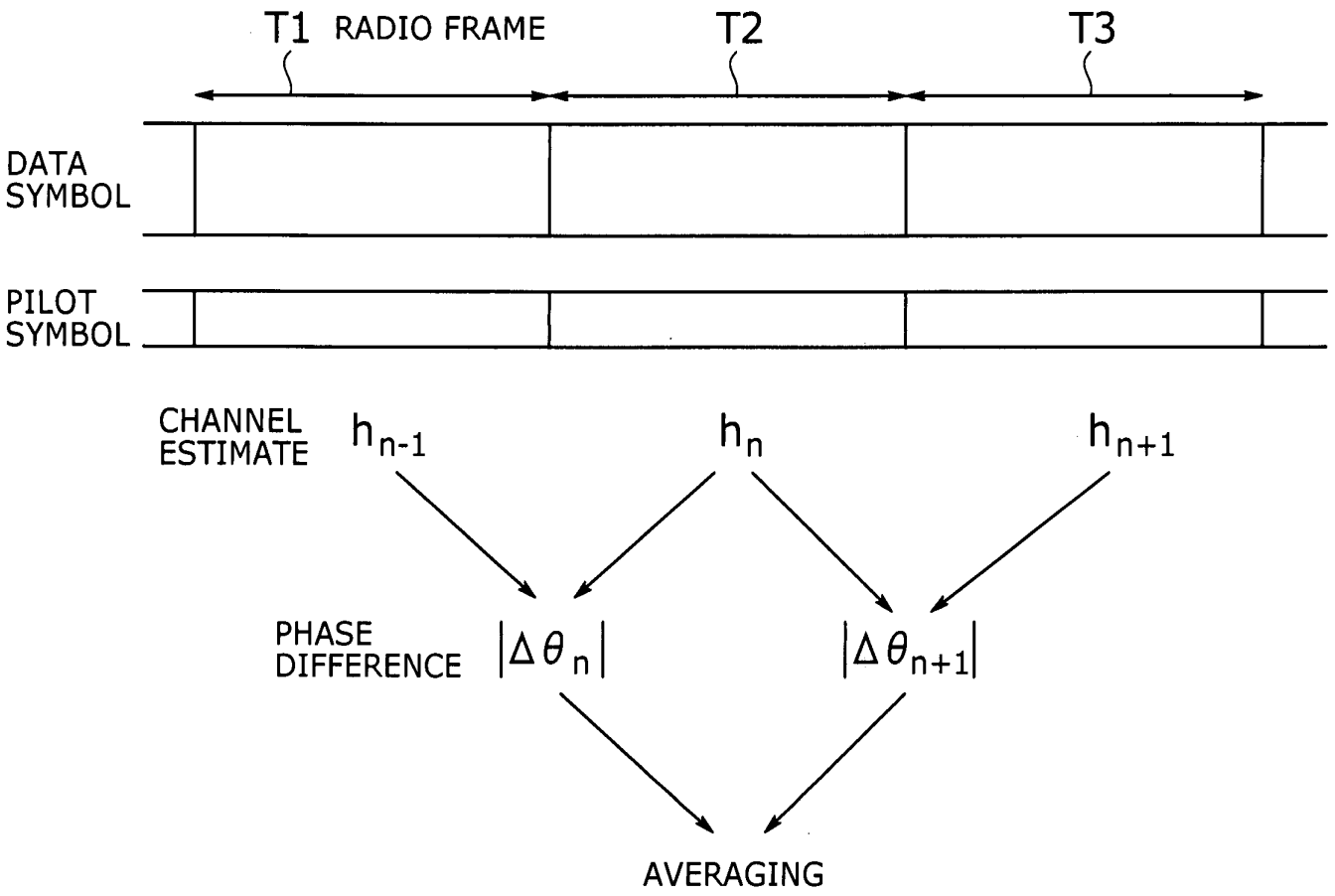

PRIOR ART

FIG. 8

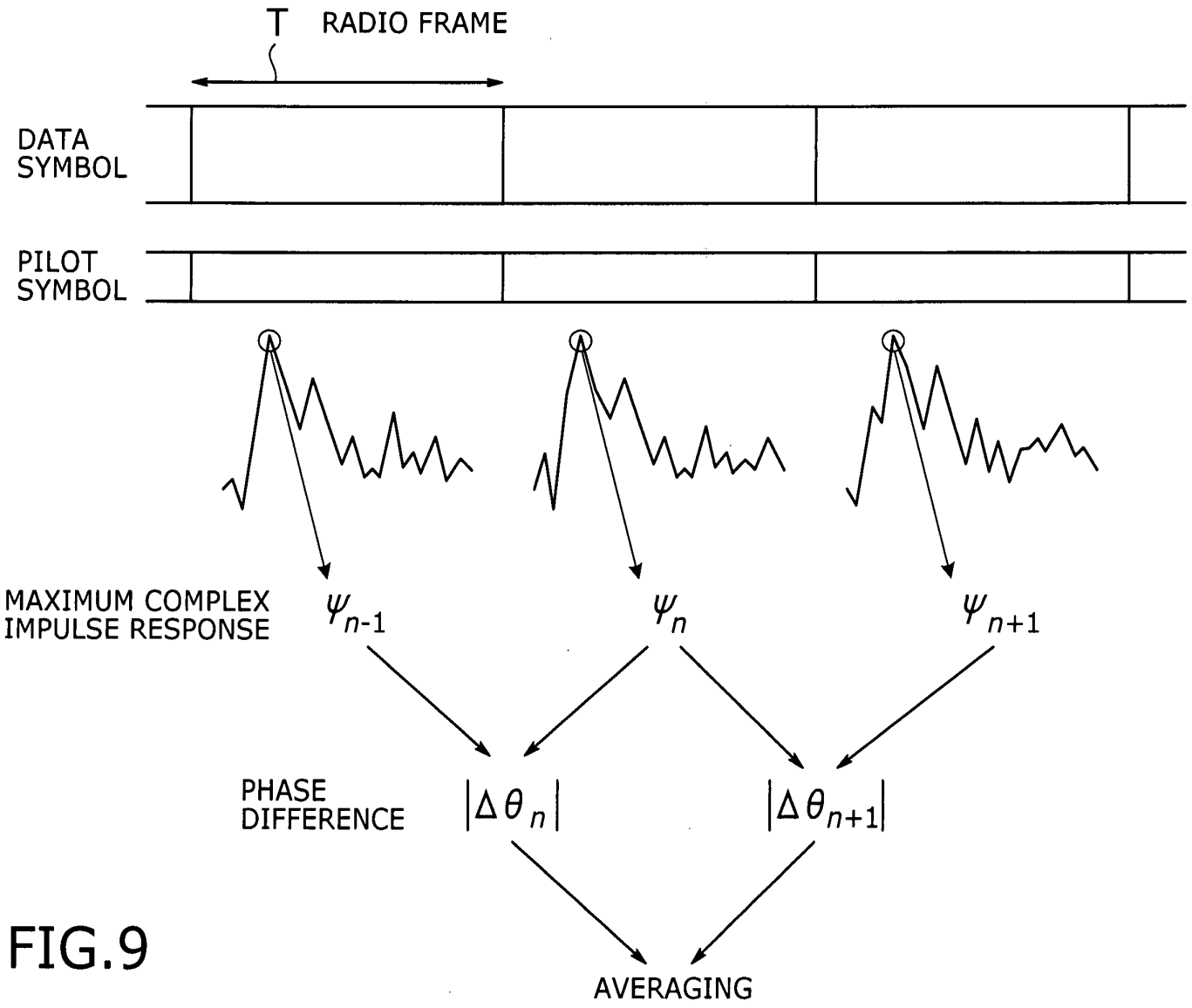
T
RADIO FRAME
DATA SYMBOL
PILOT SYMBOL
MAXIMUM COMPLEX IMPULSE RESPONSE
ψ_{n-1}
ψ_n
ψ_{n+1}
PHASE DIFFERENCE
$|\Delta\theta_n|$
$|\Delta\theta_{n+1}|$
AVERAGING

FIG.9

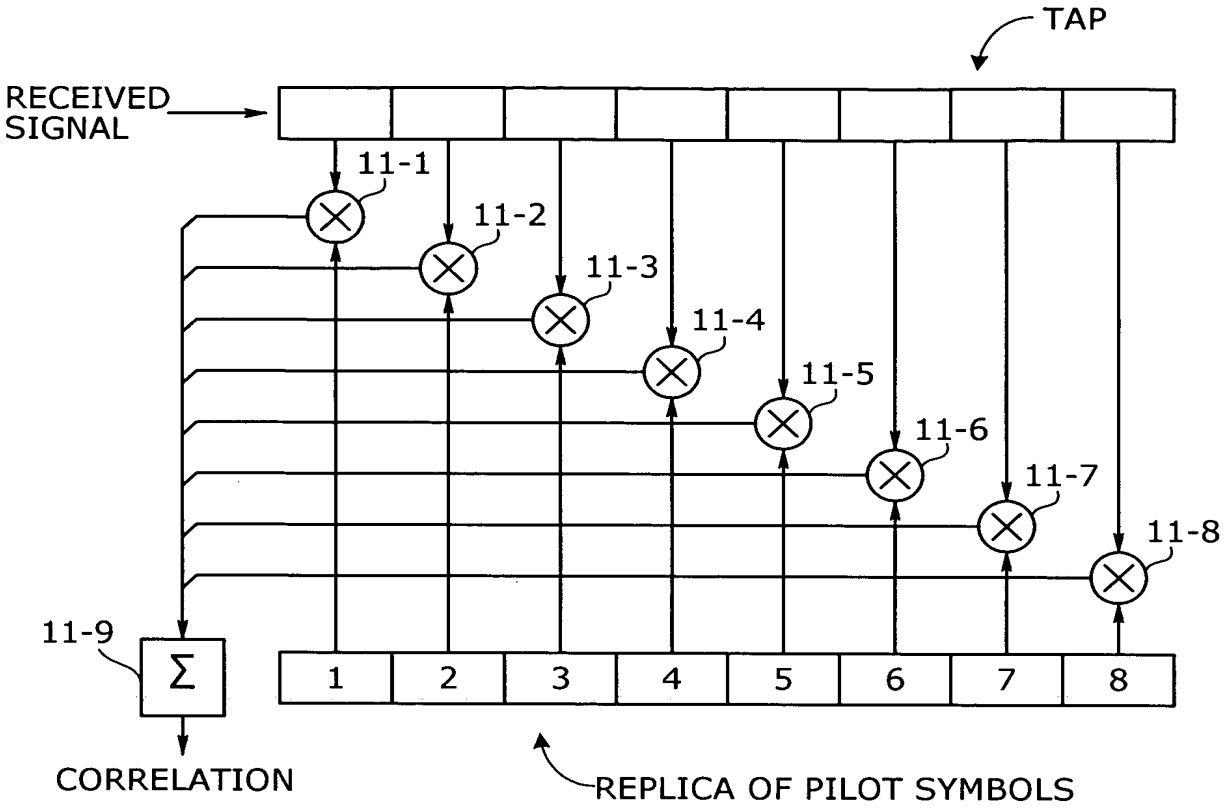

FIG. 10A

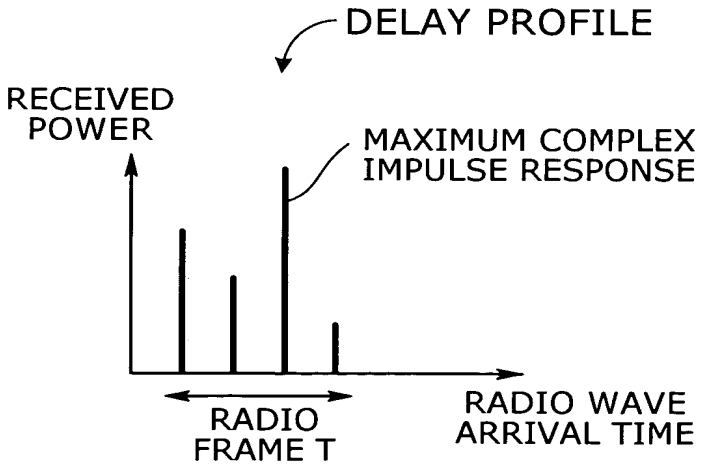

FIG. 10B

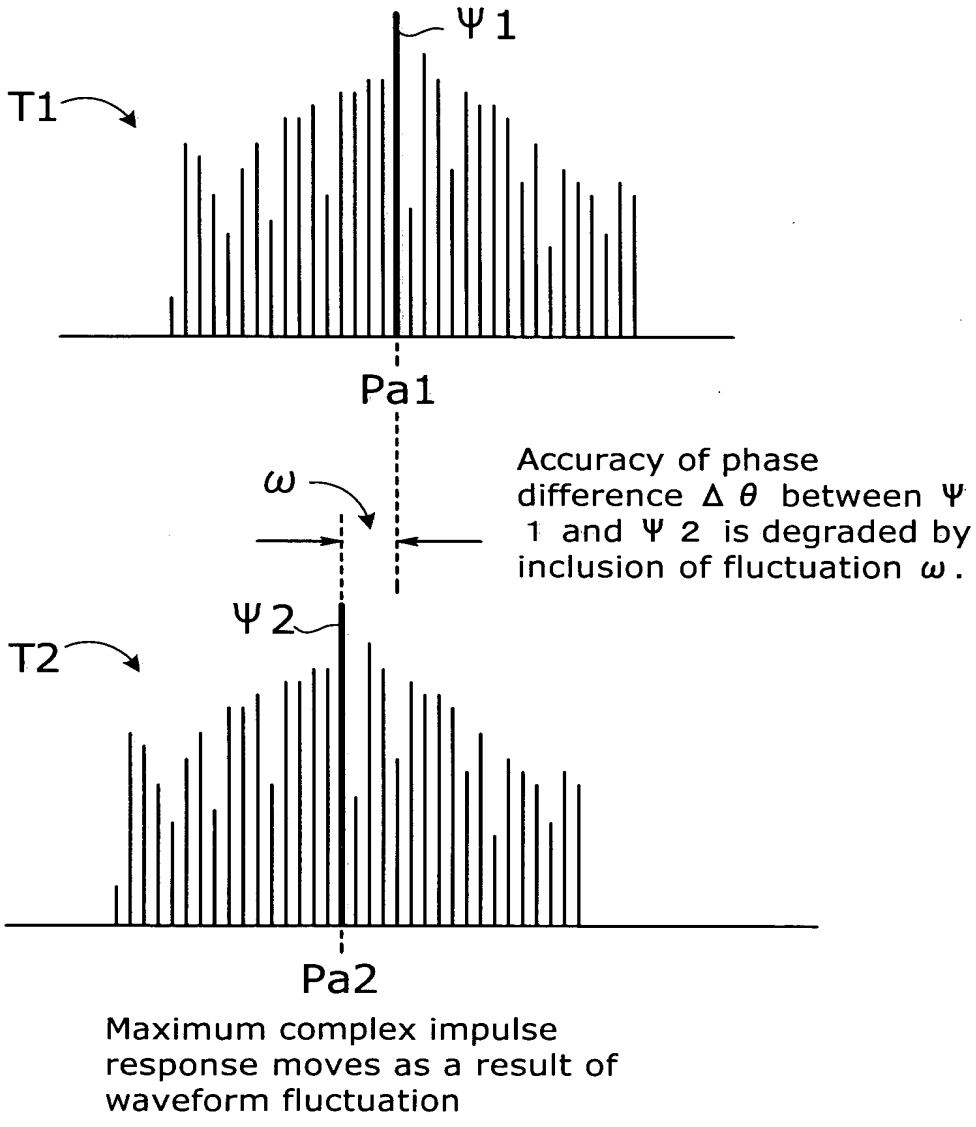
Ψ 1
T1
Pa1
ω
Accuracy of phase difference Δ θ between Ψ 1 and Ψ 2 is degraded by inclusion of fluctuation ω .
Ψ 2
T2
Pa2
Maximum complex impulse response moves as a result of waveform fluctuation

FIG. 11

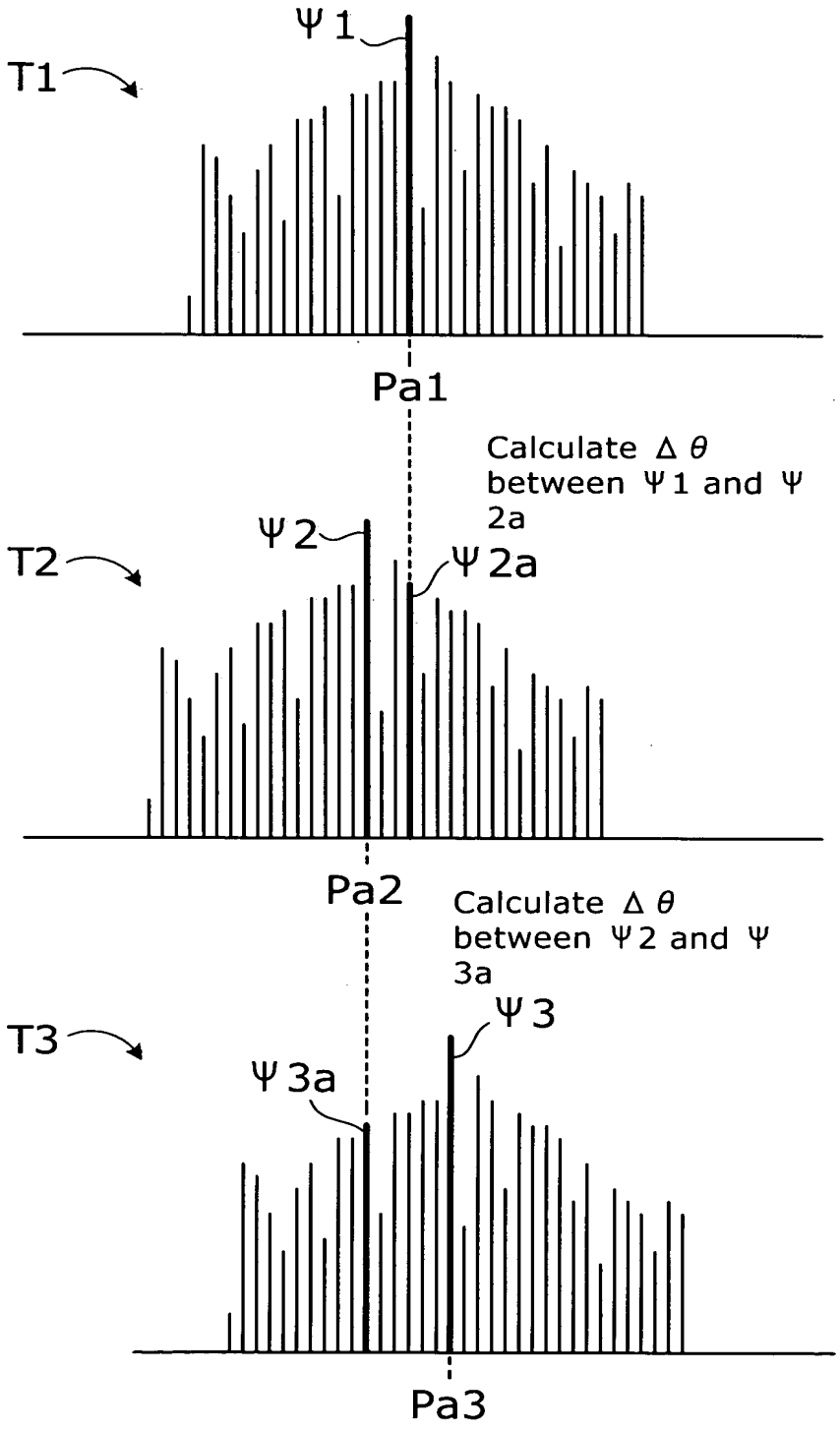
Ψ1
T1
Pa1
Calculate Δθ between Ψ1 and Ψ2a
Ψ2
Ψ2a
T2
Pa2
Calculate Δθ between Ψ2 and Ψ3a
Ψ3
Ψ3a
T3
Pa3

FIG. 12

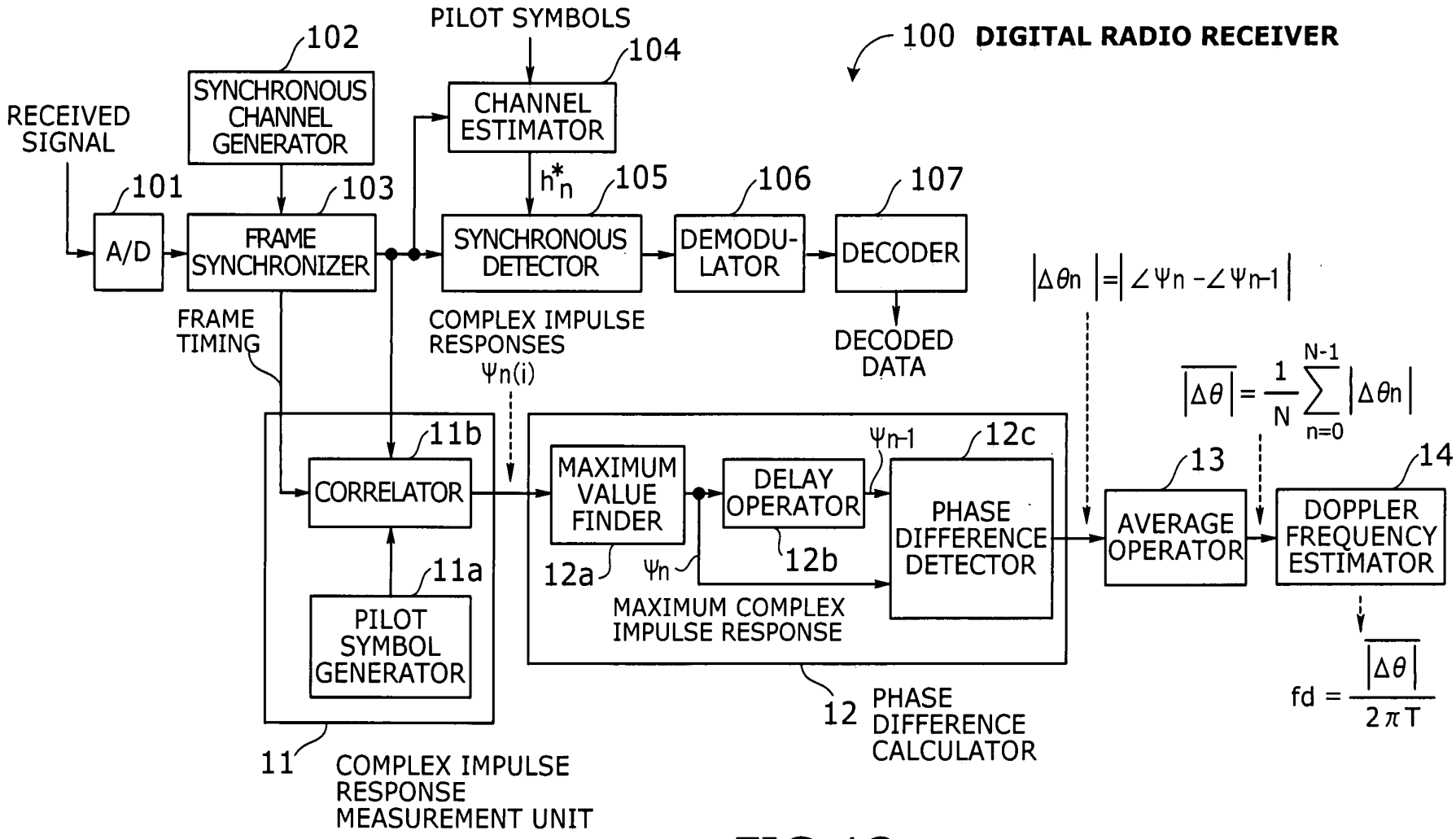
100 DIGITAL RADIO RECEIVER
RECEIVED SIGNAL
101
A/D
102
SYNCHRONOUS CHANNEL GENERATOR
103
FRAME SYNCHRONIZER
FRAME TIMING
PILOT SYMBOLS
104
CHANNEL ESTIMATOR
h*n
105
SYNCHRONOUS DETECTOR
COMPLEX IMPULSE RESPONSES
Ψn(i)
106
DEMODU-LATOR
107
DECODER
DECODED DATA
|Δθn| = |∠Ψn - ∠Ψn-1|
11b
CORRELATOR
11a
PILOT SYMBOL GENERATOR
11
COMPLEX IMPULSE RESPONSE MEASUREMENT UNIT
MAXIMUM VALUE FINDER
12a
Ψn
DELAY OPERATOR
12b
Ψn-1
12c
PHASE DIFFERENCE DETECTOR
MAXIMUM COMPLEX IMPULSE RESPONSE
12
PHASE DIFFERENCE CALCULATOR
13
AVERAGE OPERATOR
14
DOPPLER FREQUENCY ESTIMATOR
$\overline{|\Delta\theta|} = \frac{1}{N}\sum_{n=0}^{N-1}|\Delta\theta n|$
$fd = \frac{\overline{|\Delta\theta|}}{2\pi T}$

FIG.13

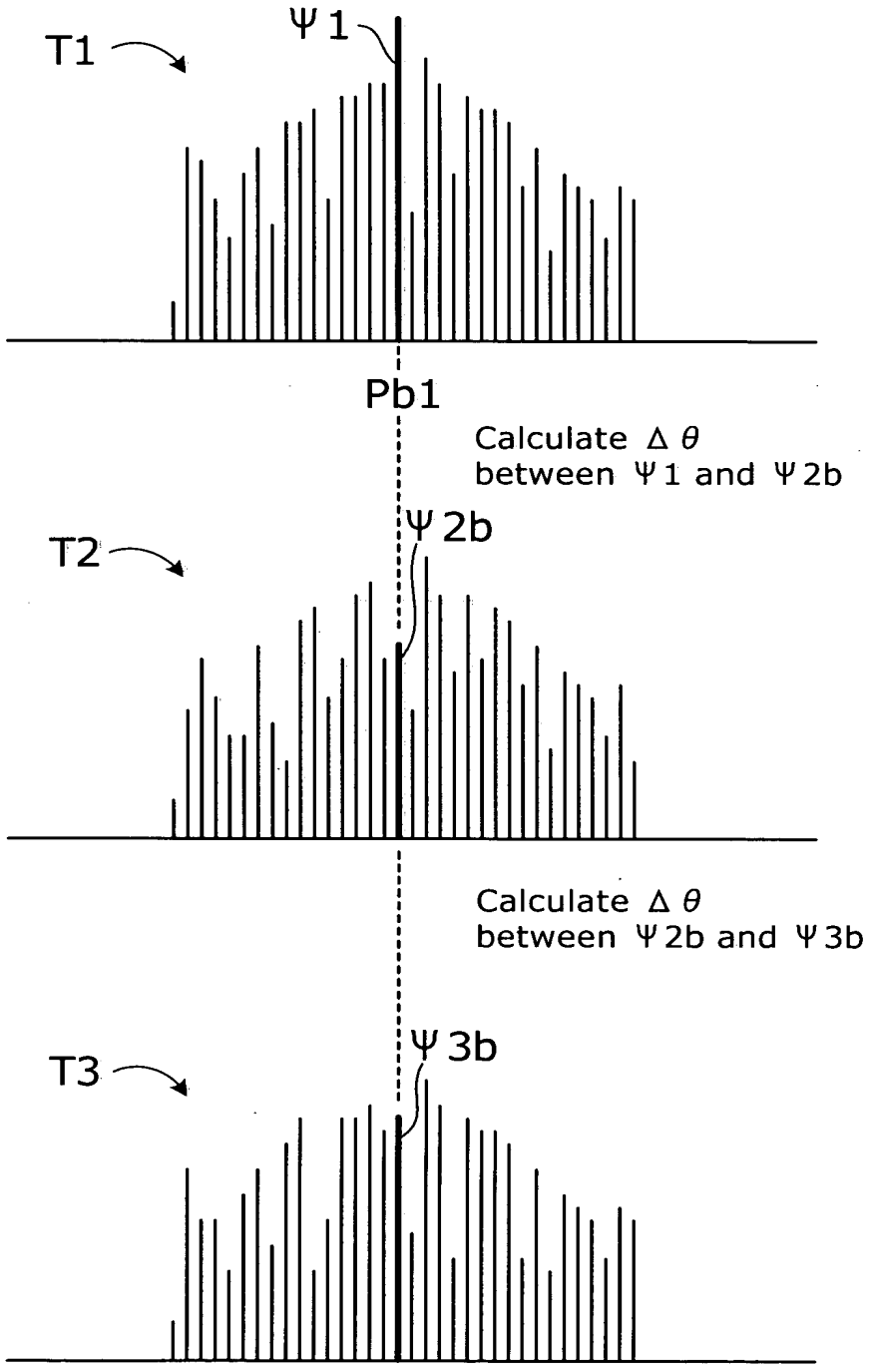
T1
Ψ1
Pb1
Calculate Δθ
between Ψ1 and Ψ2b
T2
Ψ2b
Calculate Δθ
between Ψ2b and Ψ3b
T3
Ψ3b

FIG. 14

FIG. 15A

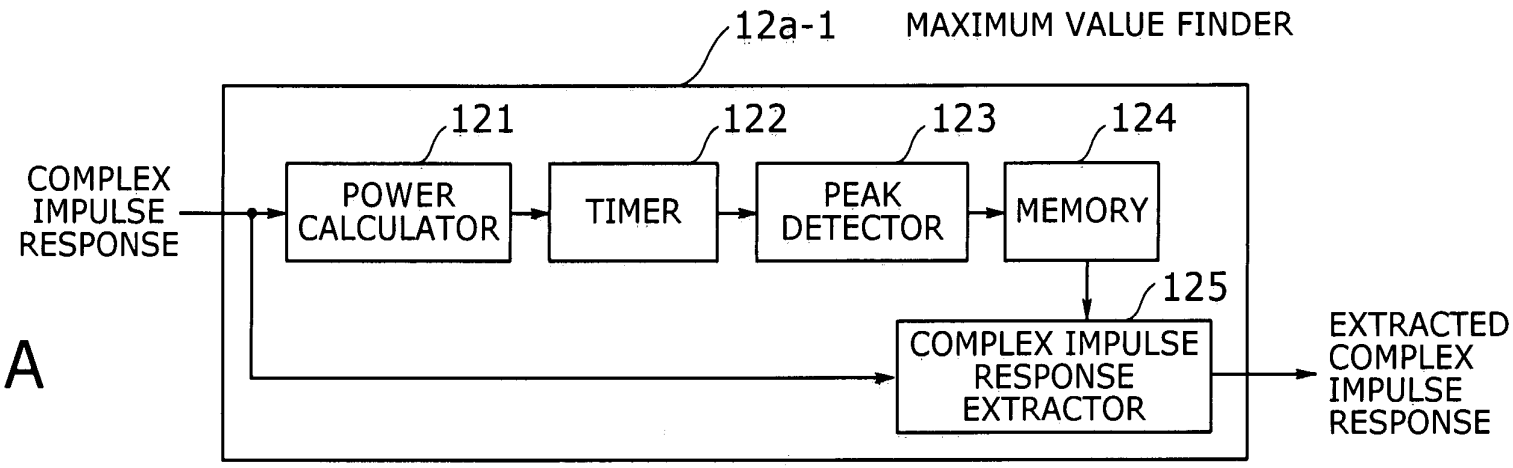

FIG. 15B

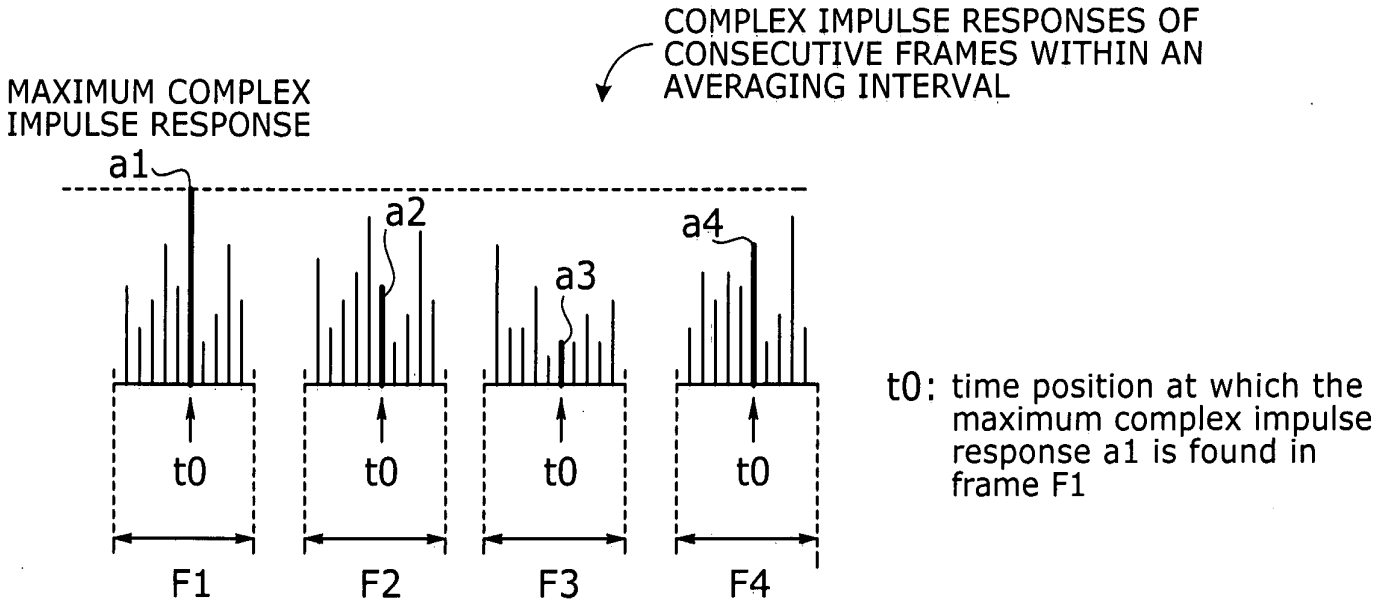

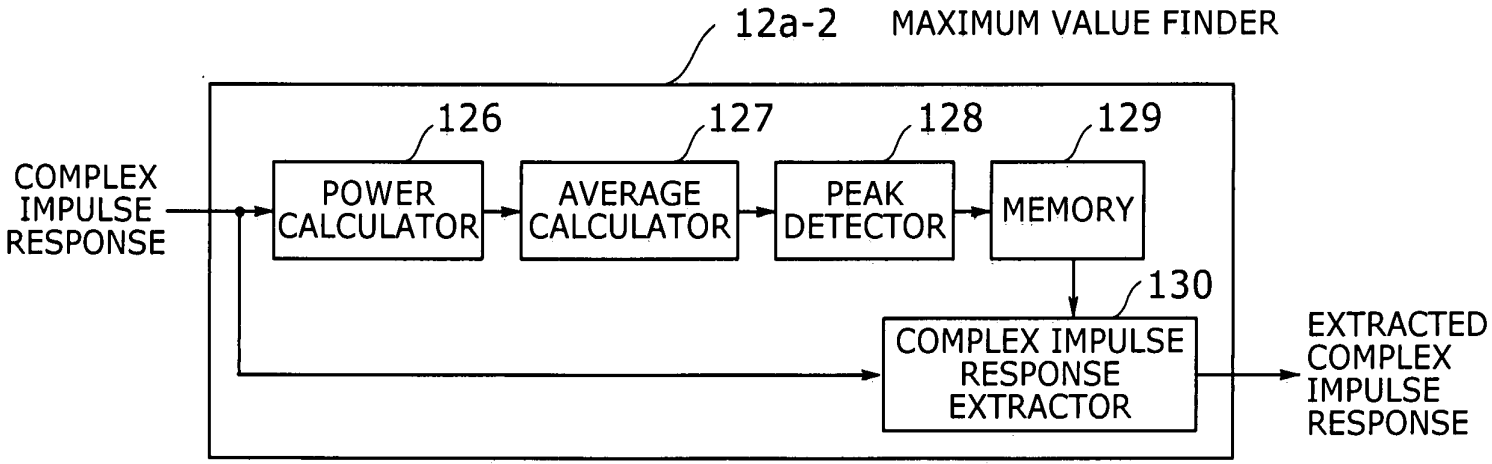
12a-2
MAXIMUM VALUE FINDER
126
127
128
129
COMPLEX IMPULSE RESPONSE
POWER CALCULATOR
AVERAGE CALCULATOR
PEAK DETECTOR
MEMORY
130
COMPLEX IMPULSE RESPONSE EXTRACTOR
EXTRACTED COMPLEX IMPULSE RESPONSE

FIG.16

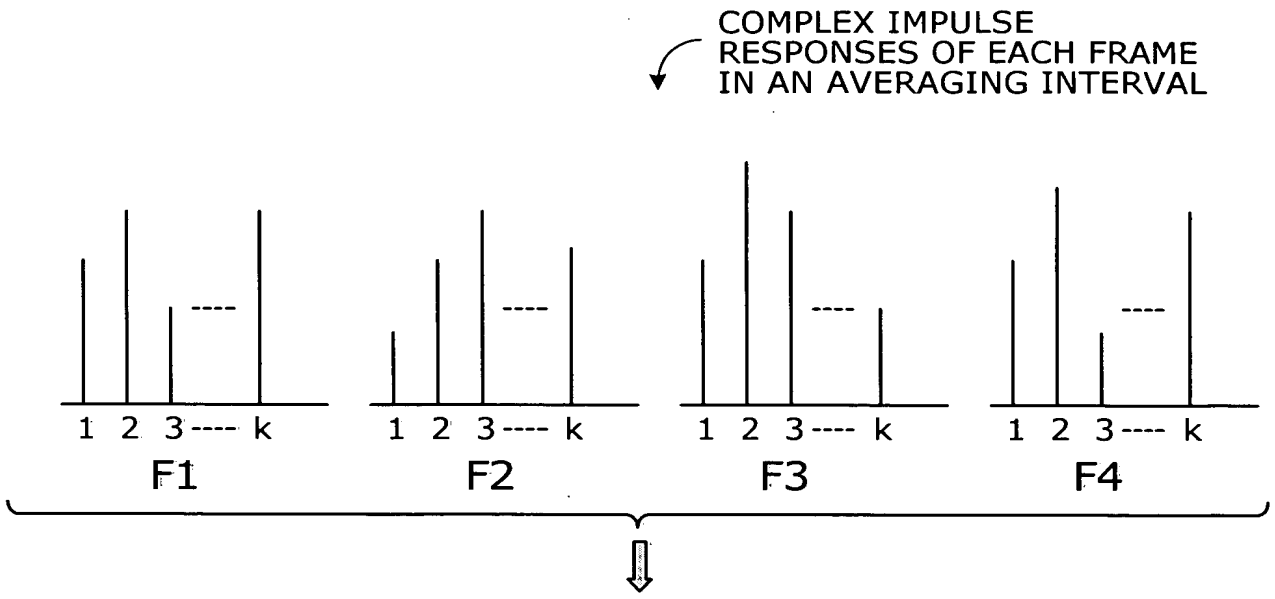

$$\phi(1) = \left(\Psi_1(1)^2 + \Psi_2(1)^2 + \Psi_3(1)^2 + \Psi_4(1)^2\right) \div 4$$

$$\phi(2) = \left(\Psi_1(2)^2 + \Psi_2(2)^2 + \Psi_3(2)^2 + \Psi_4(2)^2\right) \div 4$$

$$\vdots \qquad \vdots \qquad \vdots$$

$$\phi(k) = \left(\Psi_1(k)^2 + \Psi_2(k)^2 + \Psi_3(k)^2 + \Psi_4(k)^2\right) \div 4$$

$$\phi_{max}(i) = \max\left\{\phi(1), \phi(2), \cdots, \phi(k)\right\}$$

If ϕmax(i)=ϕ(2), then the maximum value finder 12a-2 will selectively output complex impulse responses $\Psi_1(2)$, $\Psi_2(2)$, $\Psi_3(2)$, and $\Psi_4(2)$ located at i=2 of each frame.

FIG. 17

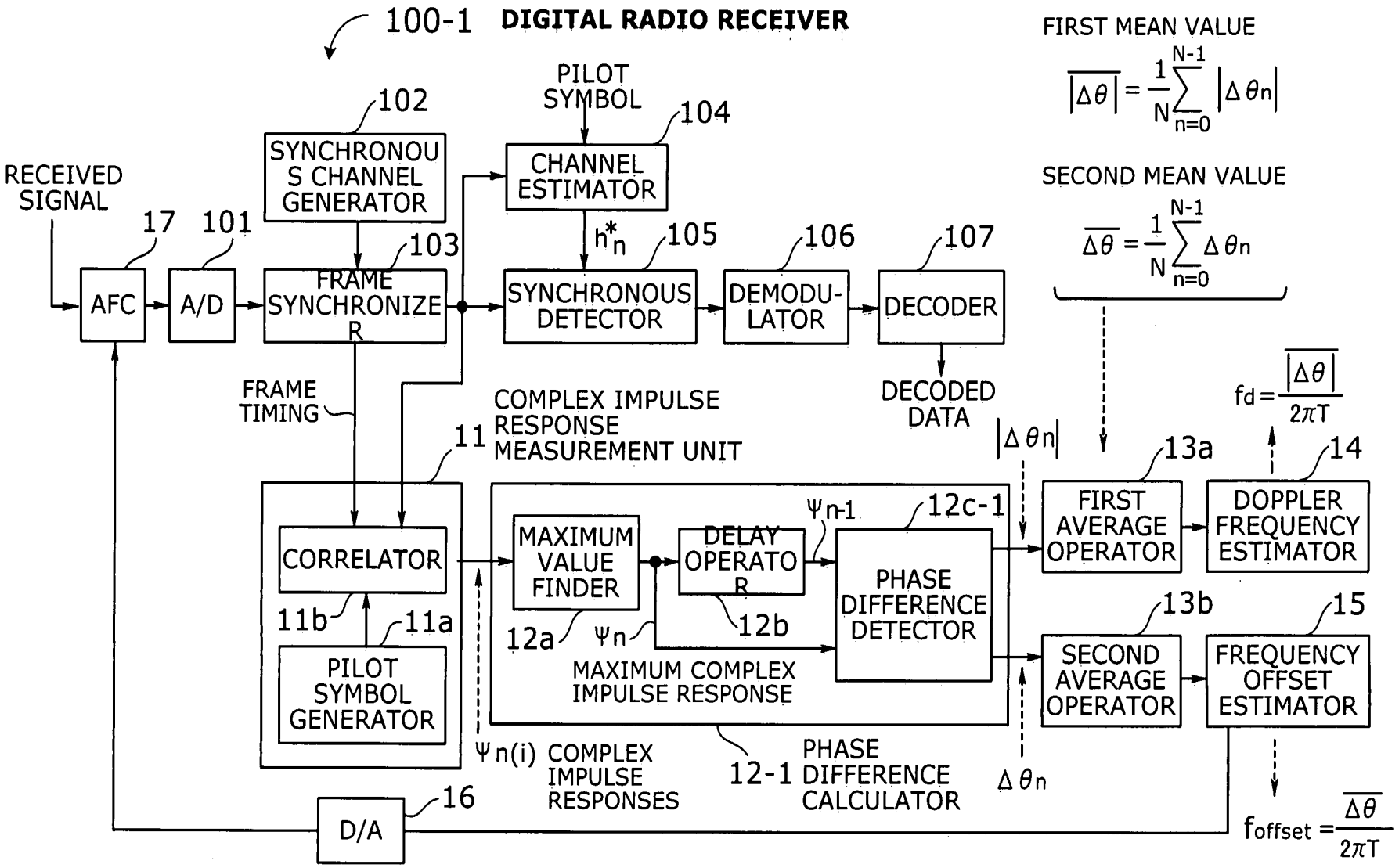
100-1 DIGITAL RADIO RECEIVER
RECEIVED SIGNAL
17
AFC
101
A/D
102
SYNCHRONOUS CHANNEL GENERATOR
103
FRAME SYNCHRONIZER
PILOT SYMBOL
104
CHANNEL ESTIMATOR
h*n
105
SYNCHRONOUS DETECTOR
106
DEMODU-LATOR
107
DECODER
DECODED DATA
FRAME TIMING
11
COMPLEX IMPULSE RESPONSE MEASUREMENT UNIT
CORRELATOR
11b
11a
PILOT SYMBOL GENERATOR
MAXIMUM VALUE FINDER
12a
DELAY OPERATOR
12b
Ψn-1
12c-1
PHASE DIFFERENCE DETECTOR
Ψn
MAXIMUM COMPLEX IMPULSE RESPONSE
Ψn(i) COMPLEX IMPULSE RESPONSES
12-1 PHASE DIFFERENCE CALCULATOR
|Δθn|
Δθn
13a
FIRST AVERAGE OPERATOR
14
DOPPLER FREQUENCY ESTIMATOR
13b
SECOND AVERAGE OPERATOR
15
FREQUENCY OFFSET ESTIMATOR
16
D/A
FIRST MEAN VALUE
$\overline{|\Delta\theta|} = \frac{1}{N}\sum_{n=0}^{N-1} |\Delta\theta n|$
SECOND MEAN VALUE
$\overline{\Delta\theta} = \frac{1}{N}\sum_{n=0}^{N-1} \Delta\theta n$
$fd = \frac{\overline{|\Delta\theta|}}{2\pi T}$
$f_{offset} = \frac{\overline{\Delta\theta}}{2\pi T}$

FIG. 18

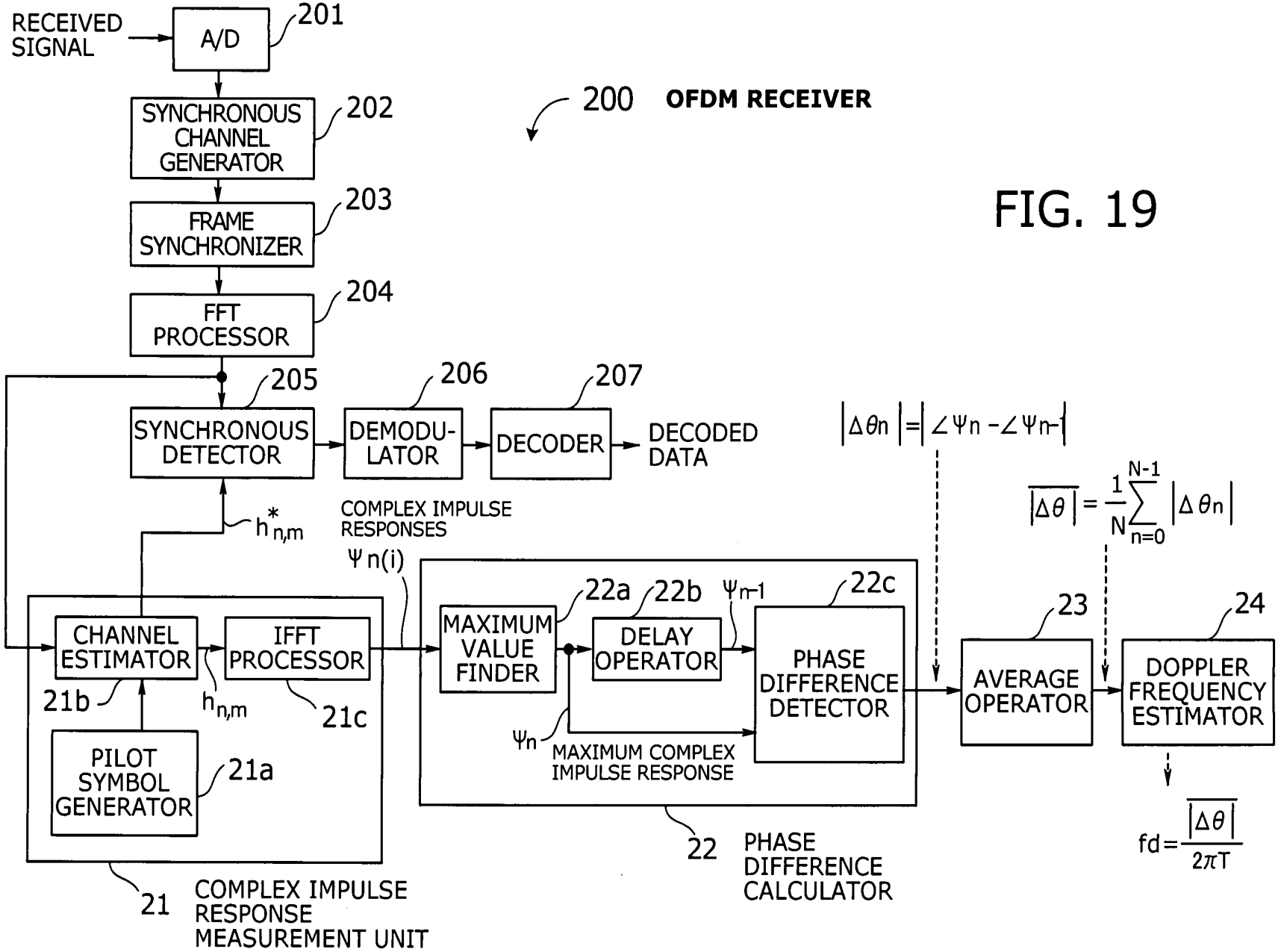
RECEIVED SIGNAL
A/D
201
SYNCHRONOUS CHANNEL GENERATOR
202
200 OFDM RECEIVER
FRAME SYNCHRONIZER
203
FFT PROCESSOR
204
205
206
207
SYNCHRONOUS DETECTOR
DEMODU-LATOR
DECODER
DECODED DATA
$|\Delta\theta n| = |\angle\Psi n - \angle\Psi n-1|$
$\overline{|\Delta\theta|} = \frac{1}{N}\sum_{n=0}^{N-1}|\Delta\theta n|$
$h^*_{n,m}$
COMPLEX IMPULSE RESPONSES
$\Psi n(i)$
22a
22b
$\Psi n-1$
22c
23
24
CHANNEL ESTIMATOR
IFFT PROCESSOR
MAXIMUM VALUE FINDER
DELAY OPERATOR
PHASE DIFFERENCE DETECTOR
AVERAGE OPERATOR
DOPPLER FREQUENCY ESTIMATOR
21b
$h_{n,m}$
21c
Ψn
MAXIMUM COMPLEX IMPULSE RESPONSE
PILOT SYMBOL GENERATOR
21a
$fd = \frac{\overline{|\Delta\theta|}}{2\pi T}$
22 PHASE DIFFERENCE CALCULATOR
21 COMPLEX IMPULSE RESPONSE MEASUREMENT UNIT

FIG. 19

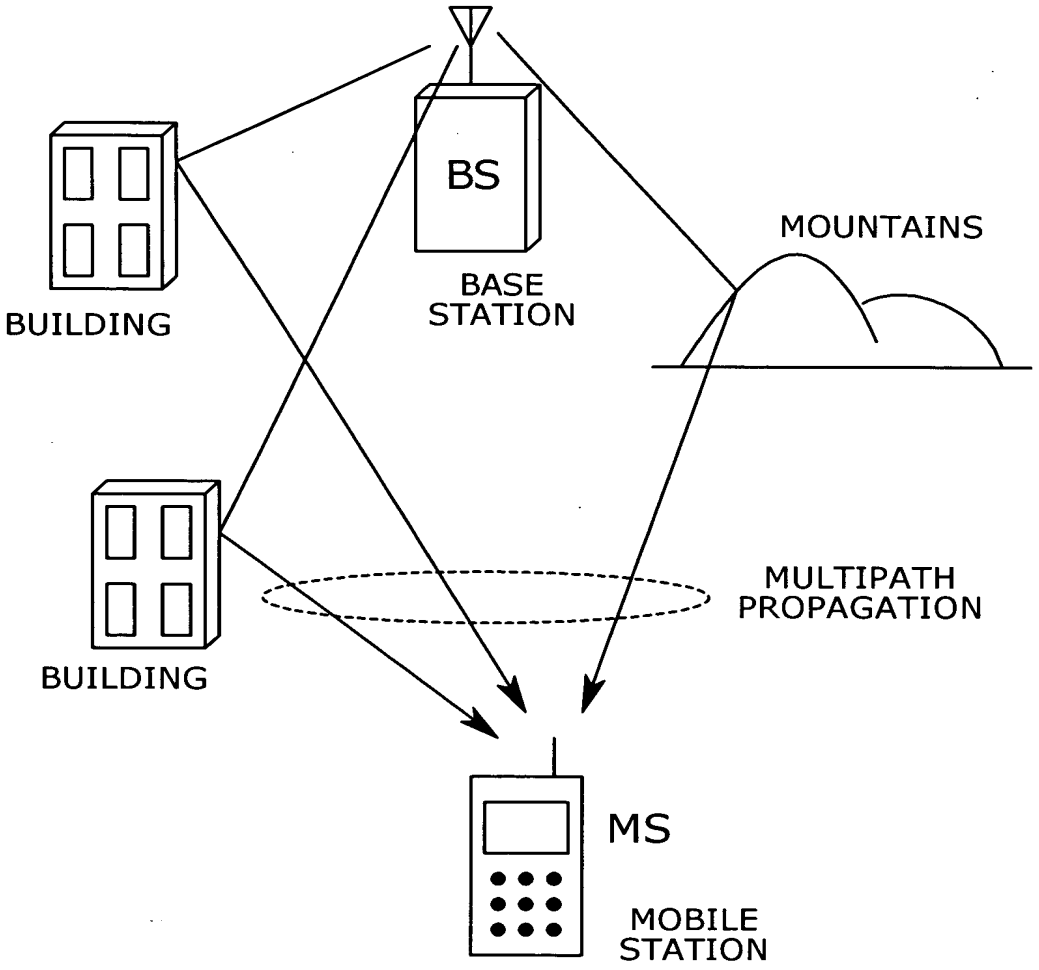
BS
BASE
STATION
MOUNTAINS
BUILDING
BUILDING
MULTIPATH
PROPAGATION
MS
MOBILE
STATION

FIG. 20